JOURNAL OF MATERIALS SCIENCE 28 (1993) 1147–1154

Sliding wear of self-mated Al_2O_3–SiC whisker-reinforced composites at 23–1200 °C

S. C. FARMER, C. DELLACORTE
National Aeronautics and Space Administration, Lewis Research Center, Cleveland, OH 44135, USA

P. O. BOOK *
Cleveland State University, Cleveland, OH 44115, USA

Microstructural changes occurring during sliding wear of self-mated Al_2O_3–SiC whisker-reinforced composites were studied using optical, scanning electron microscopy and transmission electron microscopy. Pin-on-disc specimens were slid in air at 2.7 m s^{-1} sliding velocity under a 26.5 N load for 1 h. Wear tests were conducted at 23, 600, 800 and 1200 °C. Mild wear with a wear factor of 2.4×10^{-7}–1.5×10^{-6} $mm^3 N^{-1} m^{-1}$ was experienced at all test temperatures. The composite showed evidence of wear by fatigue mechanisms at 800 °C and below. Tribochemical reaction (SiC oxidation and reaction of SiO_2 and Al_2O_3) leads to intergranular failure at 1200 °C. Distinct microstructural differences existing at each test temperature are reported.

1. Introduction

The addition of SiC whiskers to ceramic matrices has been demonstrated to enhance the material's toughness as compared to the monolith. In SiC whisker-reinforced alumina, significant increases in toughness without sacrificing strength have been obtained. The good mechanical properties of the alumina composites combined with favourable oxidation resistance has fostered continued interest in SiC whisker-reinforced alumina for use in heat engines and as cutting tools.

As improved fracture toughness can mean improved wear resistance, the potential application of alumina composite materials in high-temperature sliding components is subject to on-going investigation. Extensive research on the wear of self-mated SiC whisker-reinforced alumina has been conducted by Yust *et al.* [1] and Yust and Allard [2] at temperatures up to 800 °C in both nitrogen and air environments.

Their results of pin-on-disc sliding experiments with alumina composites show a two to four order of magnitude improvement in wear as compared to monolithic alumina. The composite wears by fracture, producing wear particles of 10–40 nm diameter. Testing results obtained in air were similar to tests in nitrogen, except at the highest temperature, 800 °C. Composite material tested at 800 °C in air developed an oxidation layer on the rubbing surface. Reduced wear was experienced. Using Auger and EDS X-ray analysis, Yust and Allard determined that the surface layer was predominantly a mixture of Al_2O_3 and SiO_2. Transmission electron microscopy revealed subsurface dislocations not observed in specimens tested at lower temperatures.

NASA has undertaken a research programme to extend study of the wear behaviour of SiC whisker-reinforced Al_2O_3 composites to temperatures as high as 1200 °C in air. We concentrated on examination of the surface and near-surface microstructural changes which occur at elevated temperatures, rather than the generated debris, as this facet of the wear problem has been less studied.

Self-mated pin-on-disc wear tests were performed at room temperature, 600, 800 and 1200 °C. The pin wear surface was then examined by scanning electron microscopy (SEM). Transmission electron microscopy (TEM) was employed to identify the microstructural changes which accompany wear at high temperatures.

2. Experimental Procedure

The composite material used in our experiments was hot-pressed high-purity alumina powder (> 99.5% purity) containing 25 vol % Tateho SiC whiskers. During hot pressing, the whiskers preferentially align perpendicular to the pressing direction. The alumina grain size is ~2 μm and the predominant defects are large whisker-free regions and voids several micrometres in diameter. These defects are visible in optical micrographs of polished cross-sections, Fig. 1.

Pins were fabricated such that the long axis of the pin is in the hot-pressing direction. Thus the whiskers

*Resident Research Associate at NASA Lewis Research Center.

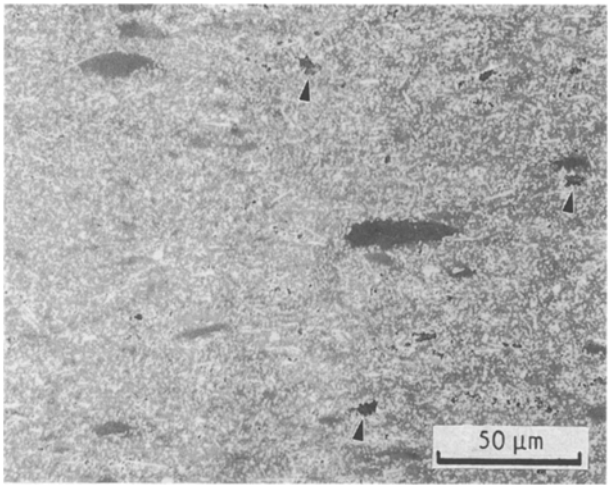

Figure 1 Optical micrograph of Al_2O_3–SiC whisker pin. Several large whisker-free regions are visible (whiskers appear white). A few of the larger voids are arrowed.

are aligned within the rubbing surface of the pin. The pins are 0.476 cm diameter by 2.5 cm. A 2.54 cm radius is machined on to the pin end and diamond polished to ~0.1 μm r.m.s. surface finish. The wear discs are 6.35 cm diameter and 1.25 cm thick with their flat faces diamond polished to ~0.1 μm r.m.s. surface finish.

Specimens were tested in a high-temperature tribometer at a sliding speed of 2.7 m s^{-1} (1000 r.p.m.) for 1 h; a total sliding distance of 9.7 km. The normal load was 26.5 N. The rig has a SiC glowbar furnace which was heated 600 °C h^{-1} to the test temperature and shut off to cool down. All tests were run in air with relative humidity from 40%–65% at 23 °C. Pin wear measurements were made by measuring the size of the flat and calculating the volume of material displaced.

In the microstructural analysis presented here, the flat worn on the pin was examined in a Cambridge 200 scanning electron microscope equipped with a Princeton Gamma Tech (PGT) energy dispersive spectrometer. Specimens for transmission electron microscopy were made by cutting a 3 mm disc from the pin wear scar. To preserve the wear surface, specimens were then polished and ion-beam milled from the opposing side to perforation. Specimens were examined on a Philips 400T equipped with an ultra thin window Kevex energy dispersive spectrometer.

3. Results

The results of the friction and wear experiments are summarized in Fig. 2. Mild wear, wear factor 2.4 $\times 10^{-7}$–1.5×10^{-6} mm^3 N^{-1} m^{-1}, occurred at all temperatures (23, 600, 800 and 1200 °C). Further details of the tribometer and tribological data on these materials have been previously reported [3, 4]. Although wear increases by a factor of about five at elevated temperatures, the increase is not monotonic. The measured wear factor was a maximum at 600 °C. A slight abatement in wear factor was measured at 800 °C. Distinct microstructural differences exist at each test temperature. These differences are discussed below.

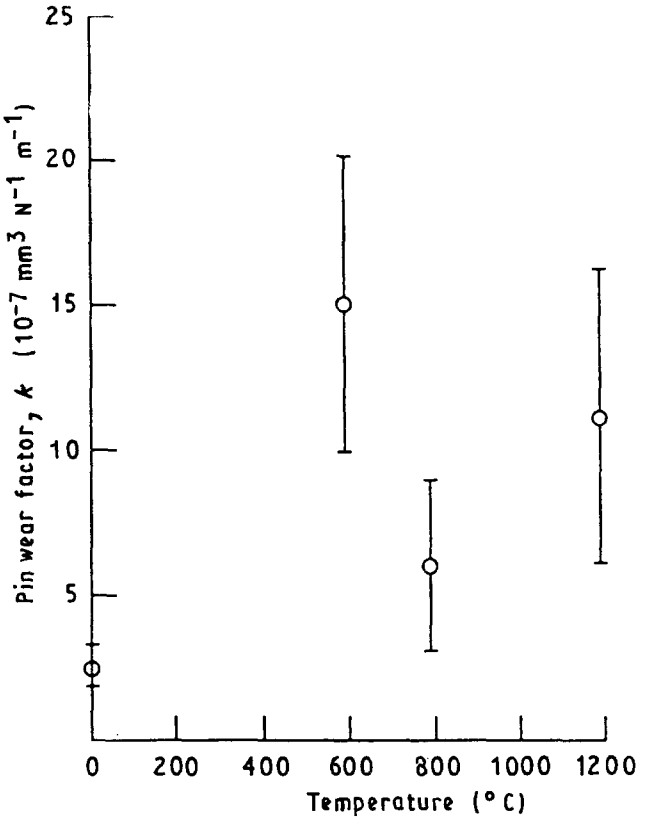

Figure 2 Plot of the wear factor, k, for the Al_2O_3–SiC composite sliding against itself in air at 2.7 ms^{-1}, 26 N load [4].

3.1. Wear at 23 °C

An SEM image of the pin wear flat is shown in Fig. 3a. The foreground is the unworn pin hemisphere. There is a ridge of compacted debris, ~5 μm high at its maximum accumulation, where the wear flat begins. Details of the debris in the flat are seen in Fig. 3b. Debris particles are equiaxed and particles ~1–5 μm diameter were measured. Examined in the TEM [4], the debris is seen to consist of alumina and SiC particles 0.2–0.5 μm in size having sharp fracture faces, Fig. 3c. In a detailed study of debris, Yust *et al.* [1] determined that debris particles visible in the SEM were actually agglomerates of much smaller particles, many less than 1μm. These authors identified the ~0.1 μm particles as being of the magnitude of asperity contacts which, once removed, are easily bonded by compressive forces. Particles agglomerate and compress to form an adherent layer. We observe considerable agglomeration consistent with Yust *et al.*'s interpretation.

A typical transmission electron micrograph of the near surface region appears in Fig. 4. The alumina grains are largely free of dislocations and in general do not contain pores. (The occasional dislocation is seen adjacent to a whisker when the whisker is located intragranularly). The whiskers are heavily faulted and contain impurity inclusions concentrated in the whisker central region. Impurities in Tateho whiskers used in this material and other commercially available whiskers have been characterized by Nutt and others [5–7]. The main metallic impurities in Tateho whiskers are 3000 p.p.m. Ca, 2400 p.p.m. Mn, 1300 p.p.m. Al, 800 p.p.m. Mg, and 500 p.p.m. Fe.

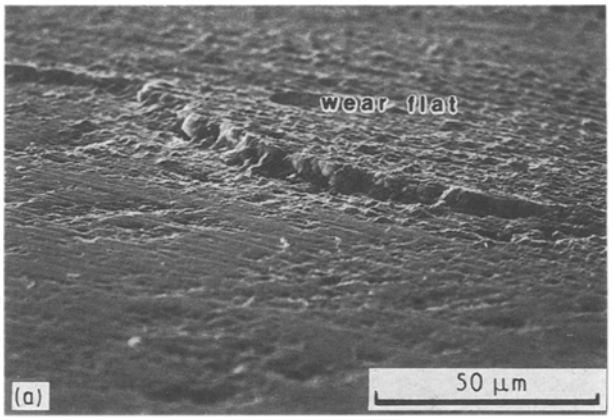

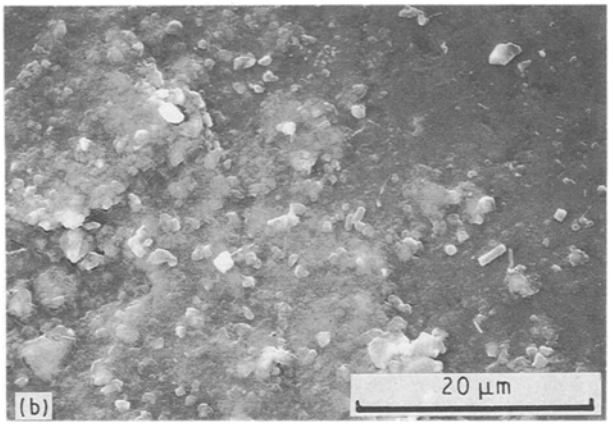

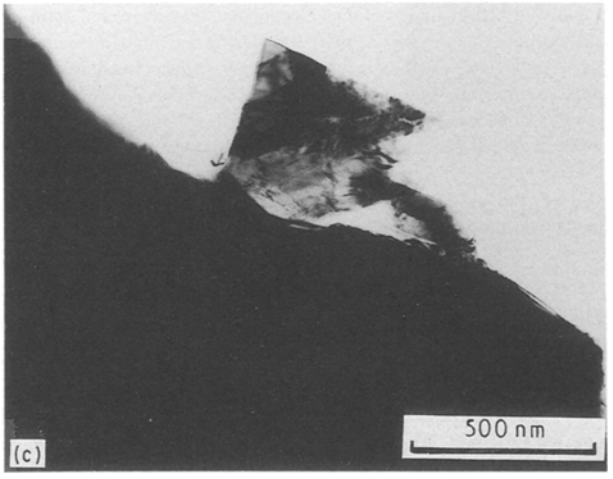

Figure 3 (a) A side view of the hemispherical pin showing the ridge of compressed and adherent wear debris (SEM). The centre of the wear flat appears in (b). Particles 1–3 μm are visible as well as large compacted flakes (lower right). (c) The transmission electron micrograph of wear debris reveals much smaller fractured particles 0.2–0.5 μm

The glassy phase at the two-grain boundaries between alumina grains is limited. However, glass is found at all triple points and at whisker agglomerates. In general, glass in Al_2O_3–SiC whisker composites arises in part from sintering aids and in part from oxidation of SiC during grinding and composite fabrication [8]. Sintering aids, however, were not used in the processing of this material. Thus the glass present derives predominantly from the added whiskers. (Also present in some intergranular regions of this material are iron silicide inclusions. The iron is

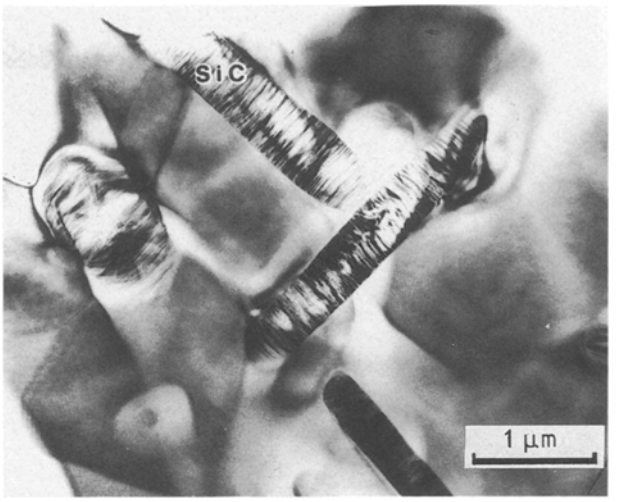

Figure 4 Transmission electron micrograph of composite pin wear tested at 23 °C. The alumina grains are free of defects. The whiskers exhibit dense stacking faults and impurity inclusions typical of the whiskers supplied.

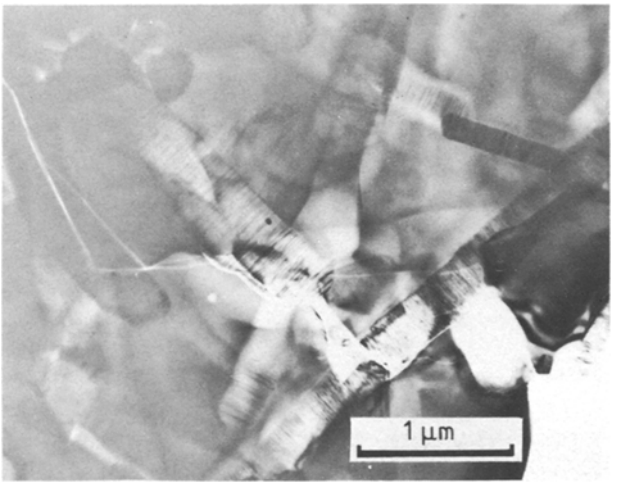

Figure 5 Transmission electron micrograph of the SiC whisker-reinforced alumina wear pin. Intra- and intergranular cracking of the alumina grains and deflection along the whisker itself is evident.

believed to originate from the steel media used in ball-milling powders. EDS analysis of such particles reveals the high iron content and associated steel alloying elements chromium, manganese and vanadium.)

Both intra- and intergranular cracking of the alumina was observed. Some deflection of the crack along the whisker also occurs, Fig. 5. Crack deflection has been described as the dominant low-temperature mechanism contributing to increased toughness [7].

3.2. Wear at 600 °C

Material is removed by brittle fracture as at lower temperatures. Fig. 6 shows a region > 10 μm in extent where material has been removed by massive intergranular fracture. Whiskers have clearly debonded and been pulled out. The fractured area is surrounded by and partially obscured by compacted debris. Directional smearing of the compacted debris is pronounced at elevated temperatures, Fig. 7a. The compacted

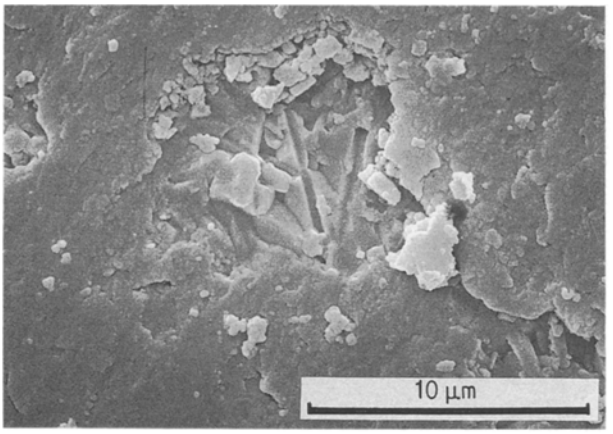

Figure 6 An SEM image of a region of recent massive fracture not yet obscured by compacted debris (600 °C wear). Depressions left by debonded whiskers are visible down the centre of the massive fracture and to the right of the centre. Debris agglomerates and compacted material surround the fracture.

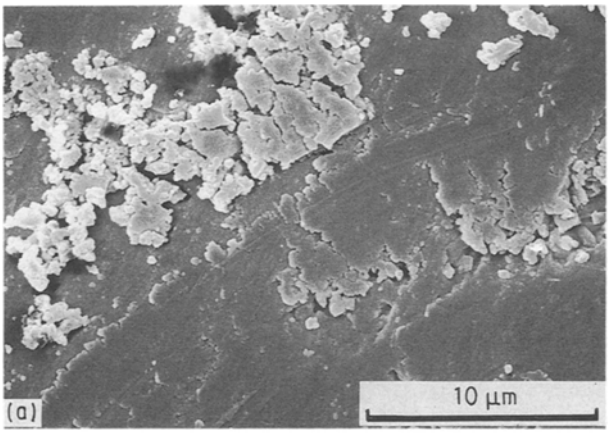

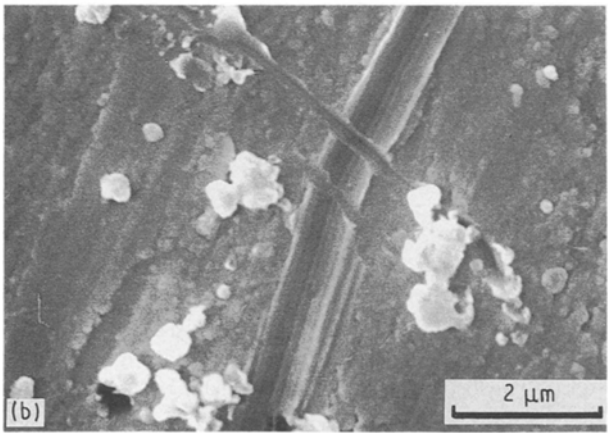

Figure 7 (a) An SEM image taken near the leading edge of the sliding surface (600 °C wear) showing initial compaction of debris agglomerates, upper right, and directional smearing of compacted debris to form a thick adherent layer. In (b) the grooving of the adherent layer by debris agglomerates is seen.

layer is soft relative to freshly generated debris and groove and lip formation occurs, Fig. 7b. The ridge between the pin wear flat and the unworn hemispherical surface of the pin is shown in Fig. 8a. In addition to individual wear particles, larger agglomerates of wear particles several micrometres in diameter and

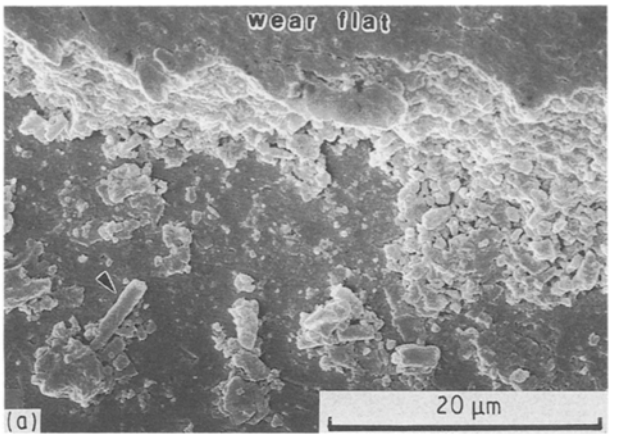

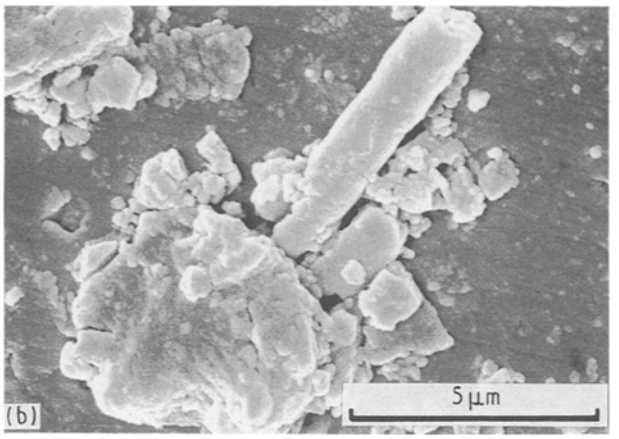

Figure 8 (a) SEM image of the ridge formed by compacted debris at the extremity of the 600 °C wear flat. The foreground shows debris particles on the machined hemispherical surface. Both very large agglomerates and cylindrical debris are apparent. An enlargement (b) shows an example of cylindrical debris ~1 μm diameter. EDS analysis of cylindrical debris usually had high Al/Si ratios. It is not clear whether cylindrical debris arises from material adhering to whisker pull-outs or occurs independently from mechanical forces in the sliding interface.

wear debris rolls are observed. The latter can be more clearly seen in the enlargement, Fig. 8b. We believe most of the wear debris rolls are whisker material plus other compacted and adhered debris.

TEM images of the 600 °C wear surface showed severe microcracking. A high dislocation density was invariably found in microcracked regions (see Fig. 9). Grains further removed from the microcracked regions contained few, if any, dislocations.

3.3. Wear at 800 °C

Although the measured wear factor was lower at 800 °C than at 600 °C, the wear surface as observed in SEM appeared very similar to the 600 °C sample. The compacted debris largely obscures the underlying surface. The debris agglomerates were larger than produced during 600 °C ambient temperature wear and somewhat more rounded. Wear debris rolls were again observed of similar diameter and length, 0.5–2.5 μm diameter and 10 μm or less in length, Fig. 10.

Numerous microstructural changes are evident in TEM. The first is the occurrence of a layer of fine mullite crystals, ~100 nm diameter, in an aluminosilicate glass, Fig. 11. Mullite formation is limited in

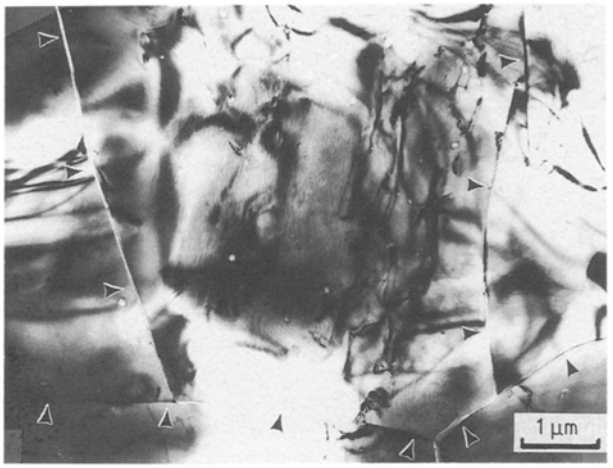

Figure 9 TEM image of the 600 °C wear surface shows extensive microcracking of the material. Cracks inclined to the surface are not as obvious as those seen "edge on" in the micrographs. Arrows have been used to make the full extent of cracking obvious. Dislocations are visible in heavily microcracked regions. Several dislocations are visible in the central region of the micrograph.

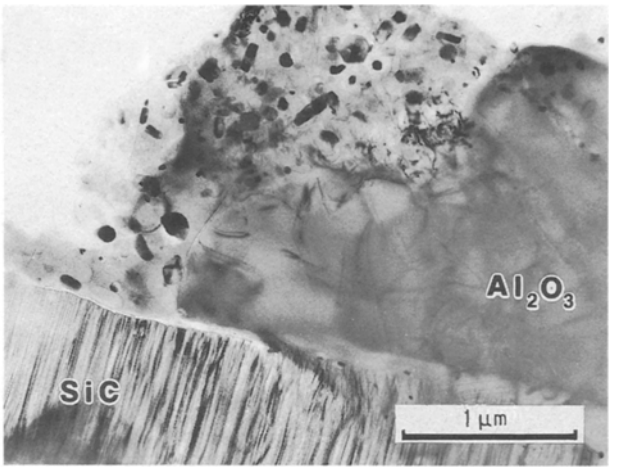

Figure 11 In TEM images of the 800 °C wear surface, mullite crystals ~100 nm are dispersed in an alumino-silicate glass (top left). An SiC whisker lying in the plane of the foil crosses the bottom of the micrograph. An alumina grain containing dislocations is seen at the right. Several such regions of small mullite crystals were found within the prepared TEM specimen.

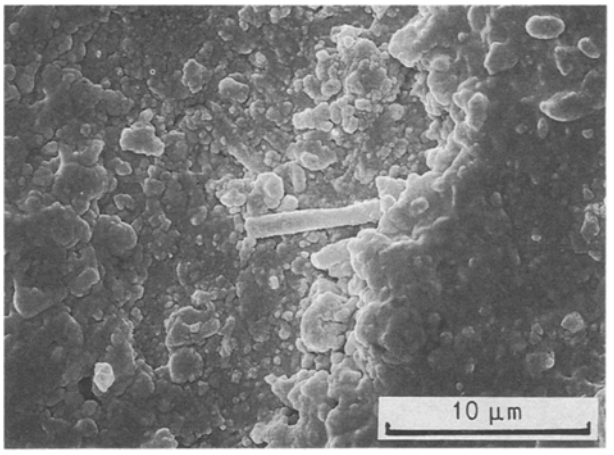

Figure 10 SEM image of compacted wear debris formed on a pin tested at 800 °C. Larger agglomerates are observed than were seen at lower temperatures. Cylindrical debris is of similar length and diameter as produced at 600 °C.

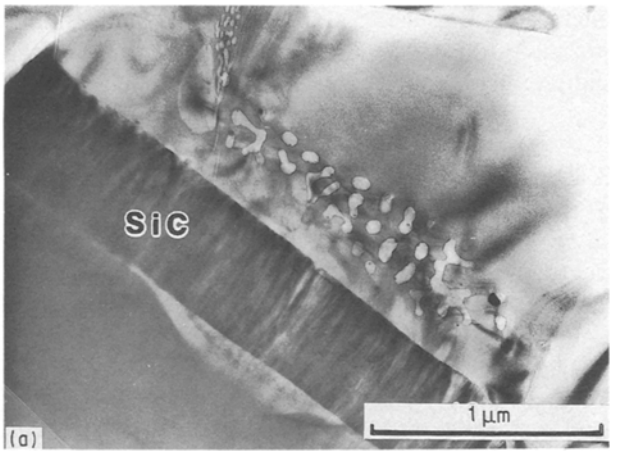

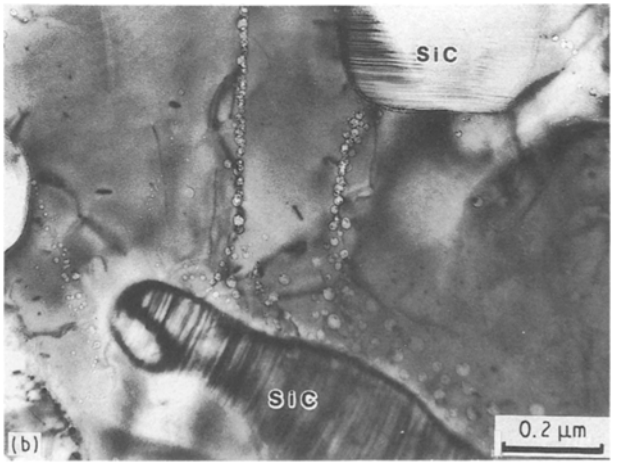

Figure 12 TEM image of crack healing captures the crack pinching off to reduce the surface area. This proceeds by ovulation – the break-up (more typically of a cylinder) into a string of spheres. Early stages of this process are shown in (a). The crack will eventually be reduced to a string of pores as seen in (b).

extent and is present at a concentration too low for detection in conventional X-ray diffractometry. Alumina grains bounded by glass are faceted. Note that dislocations are visible albeit in poor contrast in the Al_2O_3 grain. Dislocation density at the wear surface was high as was observed at 600 °C.

The most striking microstructural difference observed at the higher temperature is crack healing, Fig. 12a and b. The material appears to have extensively microcracked followed by crack healing. The healed cracks eventually form arrays of pores. Fig. 12a shows the early stages of crack healing. Fig. 12b is a later stage where a healed crack is now evidenced by a row of pores. Many pores are faceted and many contain impurity particles introduced from the wear surface and environment. The most frequently observed crystalline impurities contain zinc, copper, zirconium or lead. (The zirconium is most likely from the zirconia furnace lining. The other elements suggest a leaded brass or bronze, but no effort was made to identify a specific source.)

Regions containing healed microcracks invariably have dislocations visible under the appropriate diffraction conditions. In addition to microcracks, healed cracks, and dislocations, twinning was observed in a

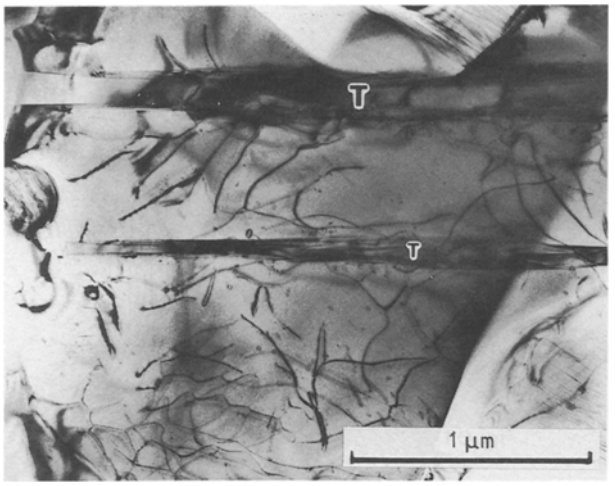

Figure 13 TEM image of an Al_2O_3 grain. Dislocations are visible, as well as two twin laths (T) which extend horizontally across the micrograph.

few grains, Fig. 13. Even at elevated temperatures, the microstructural changes observed were quite surface specific. Grains which were further away from the sliding interface ($\sim$1 mm) appear unaffected.

3.4. Wear at 1200°C

At the highest test temperature, large smears of material are visible at the leading and trailing edges of the wear flat. The ridge between accumulated debris and the hemispherical surface of the pin consists of a complex mat of glass, mullite, debris particles and whiskers, Fig. 14a and b. Debris that is thrown free of the wear scar area adheres to the pin surface and can be seen in the foreground of Fig. 14a. Detail of debris near the compacted ridge appears in Fig. 14c. Small particles a few micrometres in diameter and larger agglomerates and compacted flakes are visible. The amount of wear debris rolls has greatly increased. The length of the rolls has increased significantly. Lengths between 20 and 30 μm are now common.

Energy dispersive spectroscopy (EDS) confirms that much of the wear roll debris is whiskers. Extensive debonding of whiskers and their ejection from the sliding surface is indicated by the long lengths of such debris (up to 55 μm). Measured diameters range from 1–4 μm. The diameters are significantly greater than expected whisker diameters, indicating that adhered alumina-rich debris coats the whisker surface.

Oxidation of SiC whiskers and the resulting microstructural changes become apparent in TEM. The oxidation of SiC whiskers in Al_2O_3 matrix composites and subsequent precipitation of mullite has been effectively studied using high-resolution electron microscopy by Lin *et al.* [9]. The glass penetrates along alumina grain boundaries and reacts with the alumina. Mullite precipitates from the resulting aluminosilicate glass. The penetration of glass along alumina grain boundaries, faceting of alumina grains during alumina dissolution, and subsequent mullite precipitation produces the microstructure shown in

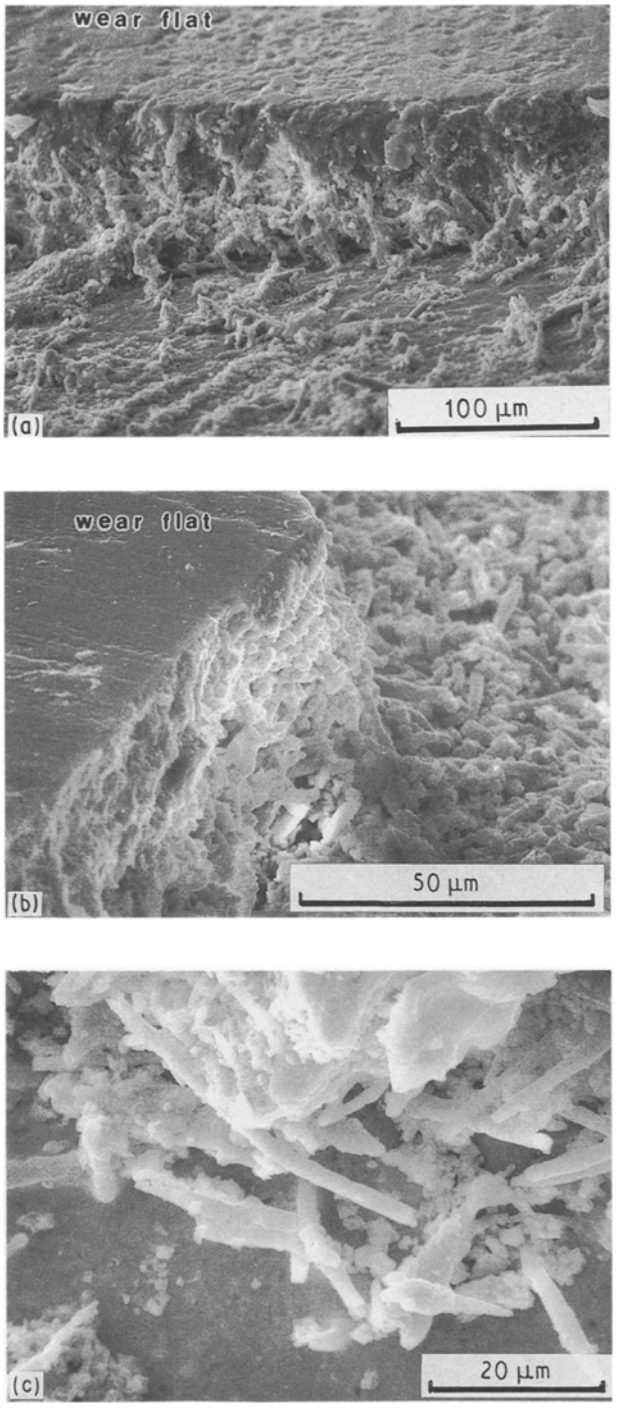

Figure 14 (a) Scanning electron micrograph of the ridge separating compacted debris from the as-machined region of the hemispherical pin. (b) Debris is larger than was seen at the lower temperatures, being ejected from the sliding surfaces before comminution. Cylindrical debris up to $\sim$55 μm in length and compacted flakes tens of micrometres in diameter (c) are observed.

Fig. 15a and b. Large regions of mullite and aluminosilicate glass exist at the surface of the 1200°C sample, Fig. 14b. Mullite formation occurs at levels detectable in X-ray diffractometry.

In sharp contrast to the 600 and 800°C samples, dislocations were not commonly observed nor was extensive microcracking in evidence. The effects of SiC-whisker oxidation (Al_2O_3 dissolution, mullite precipitation, and whisker debonding) dominate the microstructural changes during wear at 1200°C.

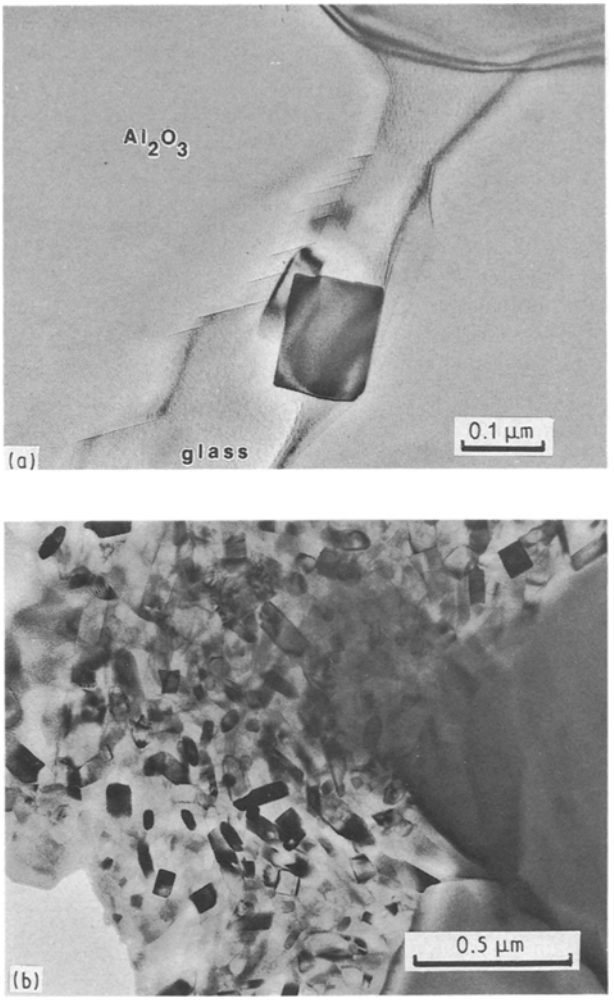

Figure 15 (a) TEM image which shows the penetration of glass into alumina grain boundaries, faceting of Al_2O_3 grains, and precipitation of mullite. The glass layer is > 100 nm thick. Prismatic mullite crystals precipitate within the intergranular glass layer. Mullite is prevalent at the wear surface. Regions of mullite plus glass, as seen in (b), are typical.

4. Discussion

The 23 °C wear sample wore by microfracture and did not exhibit other microstructural changes. Microstructural changes observed during sliding wear at elevated test temperatures, e.g. oxidation and crack healing, are well-known high-temperature phenomena. Their subsequent effect on mechanical properties has been investigated [10–13].

During sliding wear, local temperature elevation through frictional heating induces microstructure changes not generally associated with the ambient test temperatures. Griffioen *et al.* [14] observed hot-spots in unlubricated sliding surfaces and described the contact regions experiencing frictional heating as being of varied dimensions and greatly elevated temperature. In previous work, DellaCorte [15] used the model of Ashby [16] to estimate the degree of temperature elevation in pin-on-disc sliding wear. Even at moderate loads and speeds, the frictional temperatures are estimated to rise above the ambient by 400–500 °C.

The most prominent microstructural changes we observed in sliding wear of Al_2O_3–SiC whiskers composite (dislocation activity, crack healing, and SiC oxidation) are discussed below.

4.1. Dislocation activity

Wear at room temperature appears to proceed from crack initiation and growth. Few dislocations are observed. In contrast, wear at 600 and 800 °C produced massive fracture. Analysis of the dislocations generated show they arise from basal slip, $< 1120 > (0001)$. There is no indication of other active slip systems.

To satisfy von Mises' criterion for yield, five independent slip systems need be activated. Unable to deform by the conservative motion of dislocations, the material microcracks. The extension and linkage of microcracks is believed to lead to the massive fracture observed.

Contrary to initial expectations, dislocation activity was most prevalent at the intermediate ambient test temperatures of 600 and 800 °C. At the highest ambient temperature used in our studies, 1200 °C, the oxidation of whiskers initiates a series of unfavourable chemical reactions. The material fails intergranularly without generating the high stresses that can initiate dislocation activity.

4.2. SiC oxidation

Oxidation of SiC has been reported at temperatures as low as 800 °C [10] and was identified in previous 800 °C wear studies [2]. Linear oxidation rates were reported at the low temperatures. Parabolic kinetics are observed at high temperatures (> 1200 °C) where a protective SiO_2 layer forms. Oxidation in both temperature regimes is restricted to the surface regions. Where oxidation occurs, a significant increase in the incidence of whisker pull-out has been reported [11].

The glass formed during SiC oxidation penetrates boundaries reacting with the alumina grains. We observe that the SiO_2 glass formed during sliding wear at 800 and 1200 °C contains small amounts of calcium presumably from the whiskers, and a trace of sodium, a common impurity in high-grade alumina. These impurities lower the viscosity of the glass. The oxidation of SiC whiskers and subsequent reaction of the SiO_2 produced with the surrounding alumina grains facilitates extensive debonding of the whiskers during wear. Differences in thermal expansion coefficients have been advanced as a contributing factor [15].

Although SiC oxidation is anticipated during 800 °C wear, the formation of mullite at such low temperatures has not been reported. The eutectic in the Al_2O_3–SiO_2 binary system occurs at 1550 °C. Impurities substantially lower the liquidus temperature. Formation of mullite is common with many mixtures containing SiO_2 and Al_2O_3 (glazes) when fired above 1300–1350 °C. In isothermal ageing of as-received composite material, mullite was detected at similar temperatures, i.e. 1300 °C. At the isolated regions of mullite plus glass found at the 800 °C wear surface, calcium and iron were detected. The presence

of impurities and the calculated temperature increase from frictional heating of 400–500 °C appear to explain adequately mullite formation at the 800 °C ambient temperature. At a higher ambient wear temperature, 1200 °C, the reaction is no longer localized to iron-containing regions.

4.3. Crack healing

Strengthening of alumina and other ceramics through crack healing has been studied at temperatures of 1400 °C and above [12, 13, 17] Crack healing causes substantial strength recovery in thermal-shocked materials [17]. Under the conditions of frictional heating and applied pressure experienced during wear, we can observe crack healing at much lower ambient temperatures and within short times (1 h). Crack healing proceeds through several well-defined steps: (1) pinching of cracks, (2) cracks assume the shape of cylindrical voids, (3) cylindrical voids break up into numerous spherical pores.

Both glass formation through SiC oxidation and crack healing are evident in the 800 °C wear samples. Further study is needed to determine the extent to which these or other mechanisms contribute to the wear abatement at 800 °C.

4.4. Remarks

In the tests conducted, mild wear was experienced at all temperatures (23, 600, 800 and 1200 °C). We have examined microstructural changes which occur at elevated temperature and find they exert only a factor of ~ 5 change in wear rate with temperature for these very short times (1 h). Several issues are of interest for future work. These include studies of (1) wear at elevated temperatures for extended times, (2) wear at temperatures between 23 and 600 °C (Yust *et al.* [1] reported severe wear at 400 °C before a return to mild wear at 800 °C), and (3) effect of varying amounts of impurities which affect liquidus temperatures, glass softening, and glass viscosity.

5. Conclusions

Al_2O_3–SiC whisker-reinforced material was wear tested at 2.7 m s^{-1} sliding velocity under 26.5 N load for 1 h at temperatures of 23, 600, 800 and 1200 °C. The following results and conclusions were obtained.

1. Al_2O_3–SiC whisker-reinforced composites appear to be promising high-temperature wear material. Mild wear, wear factor 2.4×10^{-7}–1.5×10^{-6} mm^3 N^{-1} m^{-1}, was observed during sliding wear of self-mated Al_2O_3–SiC whisker-reinforced pin-on-disc specimens tested over the temperature range 23–1200 °C. Wear rates generally increased with temperature but at all temperatures were about an order of magnitude better than that reported for sliding wear of monolithic Al_2O_3.

2. The wear of these materials is dominated by microfracture at low ambient temperatures, 23 and 600 °C.

3. The frictional heating experienced during pin-on-disc wear induces extensive microstructural changes not otherwise observed at the ambient test temperatures. Whisker oxidation, the associated glass penetration of the alumina grain boundaries, and whisker debonding control wear at 1200 °C. A more complex combination of mechanisms contribute to wear at the intermediate temperature of 800 °C.

4. While wear rates generally increase at elevated temperatures, there is a possible abatement in wear rate at ~ 800 °C where both glass formation through SiC oxidation and crack healing are evident.

5. Although wear rates remain favourably low at elevated temperature over test times of 1 h, microstructural changes occur which may have significant effect on the wear properties over extended times and need to be considered.

References

1. C. S. YUST, J. M. LEITNAKER and C. E. DEVORE, Wear **122** (1988) 151.
2. C. S. YUST and L. F. ALLARD, *Tribology Trans.* **32** (1989) 331.
3. H. E. SLINEY and C. DELLACORTE, NASA TM-102405 (1989).
4. C. DELLACORTE, S. C. FARMER and P. O. BOOK, NASA TM-102549 and "Tribology of Composite Materials", (ASM, Materials Park, OH, 1990) p. 345.
5. S. R. NUTT, *J. Amer. Ceram. Soc.* **71** (1988) 149.
6. K. R. KARASEK, S. A. BRADLEY, J. T. DONNER, M. R. MARTIN, K. L. HAYNES and H. C. YEH, *J. Mater. Sci.* **24** (1989) 1617.
7. J. HOMENY, W. L. VAUGHN and M. K. FERBER, *J. Amer. Ceram. Soc.* **73** (1990) 394.
8. M. FALK and S. KARUNANITHY, *Mater. Sci. Engng A* **114** (1989) 209.
9. F. LIN, T. MARIEB, A. MORRONE and S. NUTT, in "High Temperature/High Performance Composites", edited by F. D. Lemhey, S. G. Fishman, A. G. Evans and I. R. Strife, MRS Symposium Proceedings, Vol. 120 (Materials Research Society, Pittsburgh, PA, 1988) p. 323.
10. S. R. NUTT, P. LIPETZKY and P. F. BECHER, Mater. Sci. Engng A **126** (1990) 165.
11. P. F. BECHER, P. ANGELINI, W. H. WARWICK and T. N. TIEGS, J. Amer. Ceram. Soc. **73** (1990) 91.
12. T. K. GUPTA, in "Structure and Properties of MgO and Al_2O_3Ceramics", edited by W. D. Kingery, Advances in Ceramics, Vol. 10 (American Ceramic Society, Columbus, OH, 1984) p. 750.
13. T. K. GUPTA, *J. Amer. Ceram. Soc.* **59** (1976) 259.
14. J. A. GRIFFIOEN, S. BAIR and W. O. WINER, in "Mechanisms and Surface Distress", Proceedings of the 12th Leeds–Lyon Symposium, edited by D. Dowson, C. M. Taylor, M. Godet and D. Berthe (Butterworths, London, 1986) p. 238.
15. C. DELLACORTE, NASA TM-103799 (1991).
16. M. F. ASHBY, in "Modelling of Wear in Energy Conversion and Utilization Technologies", June 1989 US DOE, ANL Div. of Ed. Prog. Conf-8806370 Argonne, IL (1989) p. 25.
17. T. K. GUPTA, *J. Amer. Ceram. Soc.* **61** (1978) 191.

Received 6 August 1991
and accepted 7 May 1992